IN REPLY REFER TO:

UNITED STATES
DEPARTMENT OF THE INTERIOR
GEOLOGICAL SURVEY
WASHINGTON 25, D. C.

AEC - 764/6

May 16, 1956

Mr. Robert D. Nininger, Assistant Director
Division of Raw Materials
U. S. Atomic Energy Commission
Washington 25, D. C.

Dear Bob:

Transmitted herewith are three copies of TEI-481, "Exploring for ancient channels with the refraction seismograph," by L. C. Pakiser and R. A. Black, March 1956.

We are asking Mr. Hosted to approve our plan to submit this report for publication in Geophysics.

Sincerely yours,

John H. Eric

for W. H. Bradley
Chief Geologist

Geology and Mineralogy

This document consists of 35 pages
Series A

UNITED STATES DEPARTMENT OF THE INTERIOR

GEOLOGICAL SURVEY

EXPLORING FOR ANCIENT CHANNELS WITH THE REFRACTION SEISMOGRAPH*

By

L. C. Pakiser and R. A. Black

March 1956

Trace Elements Investigations Report 481

This preliminary report is distributed without editorial and technical review for conformity with official standards and nomenclature. It is not for public inspection or quotation.

*This report concerns work done on behalf of the Division of Raw Materials of the U. S. Atomic Energy Commission.

USGS - TEI-481

GEOLOGY AND MINERALOGY

Distribution (Series A)	No. of copies
Atomic Energy Commission, Washington.	2
Division of Raw Materials, Albuquerque.	1
Division of Raw Materials, Austin	1
Division of Raw Materials, Butte.	1
Division of Raw Materials, Casper	1
Division of Raw Materials, Denver	1
Division of Raw Materials, Ishpeming.	1
Division of Raw Materials, Phoenix.	1
Division of Raw Materials, Rapid City	1
Division of Raw Materials, St. George	1
Division of Raw Materials, Salt Lake City	1
Division of Raw Materials, Washington	3
Exploration Division, Grand Junction Operations Office. . . .	6
Grand Junction Operations Office.	1
Technical Information Extension, Oak Ridge.	6
U. S. Geological Survey:	
Fuels Branch, Washington.	1
Geochemistry and Petrology Branch, Washington	1
Geophysics Branch, Washington	6
Mineral Deposits Branch, Washington	1
P. C. Bateman, Menlo Park	1
A. L. Brokaw, Grand Junction.	2
N. M. Denson, Denver.	1
V. L. Freeman, College.	1
R. L. Griggs, Albuquerque	1
M. R. Klepper, Spokane.	1
A. H. Koschmann, Denver	1
J. D. Love, Laramie	1
L. R. Page, Washington.	1
Q. D. Singewald, Beltsville	1
A. E. Weissenborn, Spokane.	1
TEPCO, Denver	2
TEPCO, RPS, Washington, (including master).	3
	54

CONTENTS

ILLUSTRATIONS

EXPLORING FOR ANCIENT CHANNELS WITH THE REFRACTION SEISMOGRAPH

By L. C. Pakiser and R. A. Black

ABSTRACT

In the Monument Valley of Arizona and Utah, uranium ore has been found in ancient channel deposits, primarily in the Shinarump member of the Chinle formation of Late Triassic age. The seismic velocity in the Shinarump member is substantially less than that in the Moenkopi formation of Early and Middle (?) Triassic age, which unconformably underlies the Shinarump. Therefore, the ancient channels can be located by using the refraction seismograph. Because the erosion surface of the Moenkopi in channel areas is curved, a delay time method of analysis is used to determine the position in depth of the Shinarump and Moenkopi contact. The problem of velocity variations within the Shinarump can be largely overcome by careful interpretation supported by drill-hole and velocity control.

INTRODUCTION

In the Monument Valley of Arizona and Utah uranium ore has been found in ancient channel deposits. Stream channels cut into the Moenkopi formation of Early and Middle (?) Triassic age were filled with the basal sediments of the Shinarump member of the Chinle formation of Late Triassic age and subsequently the Moenkopi formation was buried under the Shinarump member and younger sedimentary rocks. It is in these channel sediments of the Shinarump that the uranium ore was deposited. Not all of these ancient channels contain mineralized zones and mineralized zones may be sporadic along any channel trend, but the discovery of a channel is the first step in finding uranium ore in this area. If channels can be discovered economically by geophysical means, drilling costs can be sharply reduced.

The velocity in the coarse clastic rocks of the Shinarump member is substantially less than that in the underlying shales and mudstones of the Moenkopi formation, so that where the Shinarump is exposed at the surface or covered by a few feet of surficial deposits the unconformity on the surface of the Moenkopi can be mapped with the refraction seismograph. Special problems in refraction shooting arise, however, where the mudstones of the Chinle formation of Late Triassic age overlie the Shinarump member. The velocities in these mudstones exceed that of the Shinarump member and may approach that of the Moenkopi. Only areas where the Shinarump member is the surface rock will be discussed in the present paper.

Wantland and Casey of the U. S. Bureau of Reclamation conducted the first seismic refraction work in Monument Valley at Nokai Mesa, along the Arizona-Utah border in the Navajo Indian Reservation, during August and September 1952(Wantland and Casey, 1952; Wantland, 1954). They were able to map a large channel without difficulty and their results agreed closely with the drill-hole control.

The U. S. Geological Survey on behalf of the Division of Raw Materials of the U. S. Atomic Energy Commission began exploring for ancient channels in a number of areas in Monument Valley in the summer of 1953. In most of these areas the Shinarump and Moenkopi contact was successfully mapped, but many problems not present at Nokai Mesa had to be considered during the course of these later investigations. These problems include: (1) velocity variations in the Shinarump member, particularly the presence of high-velocity mudstone lenses; (2) velocity variations in the Moenkopi formation; and (3) irregularly curved refracting surfaces requiring special interpretation methods. Many of these problems have been successfully overcome and the seismic refraction method has been established as the most useful geophysical tool yet available in locating ancient buried channels.

This paper illustrates some of these problems and presents a method of interpreting traveltime curves in channel areas.

LOCATION AND GEOLOGY

The places in which the refraction seismograph has been used to explore for ancient channels in the Monument Valley area of Utah and Arizona are shown in figure 1. The Monument Valley area in southern Utah is bounded by the 110th meridian on the east, the San Juan River on the north, Copper Canyon on the west, and the Utah-Arizona state line on the south. In Arizona, the Monument Valley area includes the Boot Mesa, Agathla Peak, and Garnet Ridge 15-minute quadrangles. The Monument Valley area can be reached by Utah State Highway 47 from the north and by various roads through the Navajo Indian Reservation from the south.

The major structural feature of the Monument Valley area is the Monument Upwarp, which trends approximately north, and extends from Kayenta, Ariz., to the junction of the Green and Colorado Rivers in Utah. The Monument Upwarp is a broad, flattened anticline with associated subordinate folds which are usually asymmetrical. Two of these sub-

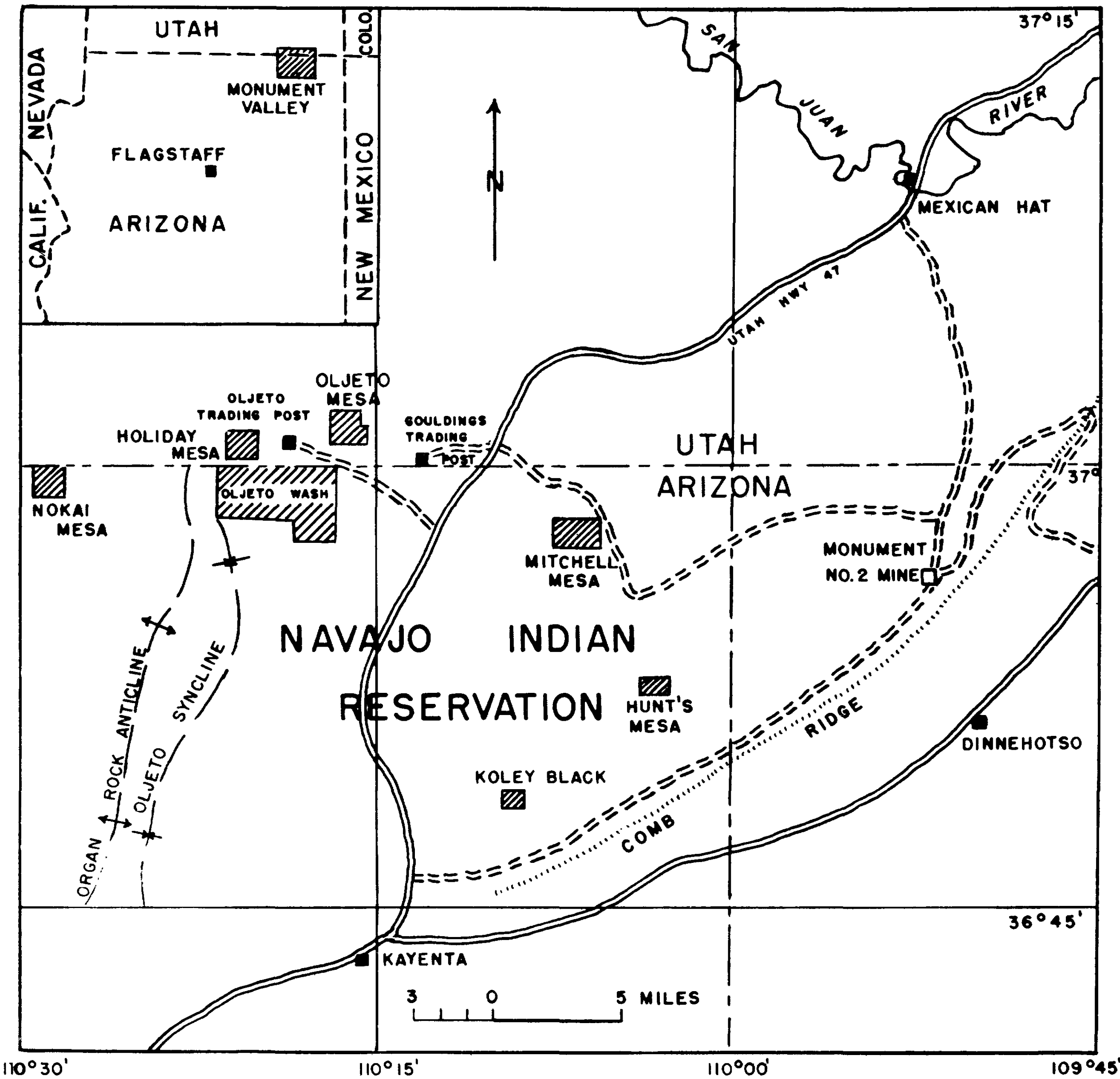

(AFTER I. J. WITKIND, 1954)

FIGURE I. MAP OF PART OF MONUMENT VALLEY AREA SHOWING LOCATIONS OF REFRACTION SEISMOGRAPH SURVEYS ordinate features are the Oljeto syncline and the Organ Rock anticline (fig. 1).

The axis of the Oljeto syncline approximately follows the course of Oljeto Wash, and the west limb of the syncline (the Hoskinini monocline) rises steeply to the Organ Rock anticline, which roughly parallels the Oljeto syncline.

In Monument Valley the exposed, consolidated, sedimentary rocks range in age from Permian to Jurassic, and their total thickness may be as much as 8,000 feet (Baker, 1936). Uranium deposits are found in many places in the Shinarump member of the Chinle formation of Late Triassic age. The Shinarump member in the Monument Valley area varies in composition from a coarse basal conglomerate to a medium- to coarse-grained sandstone in the upper part. The light gray or buff sandstone and conglomerate of the Shinarump grade into each other and are in many places cross bedded. The Shinarump contains considerable quantities of silicified wood and some black carbonaceous material. Mudstone lenses are common in the Shinarump; these lenses range in thickness from a few inches to as much as 10 feet and may have a considerable lateral extent. In the Monument Valley area, the thickness of the Shinarump ranges from a few feet to 200 feet or more in the deeper channel troughs.

The Shinarump member of the Chinle formation is underlain by the Moenkopi formation of Early and Middle (?) Triassic age. The Moenkopi is composed of dark brown to red-brown thin, evenly bedded, sandy shales and thin, ripple-marked sandstones.

The contact between the Shinarump and the Moenkopi is a widespread unconformity marked by contrasting textures and rock compositions. In places, the Shinarump and Moenkopi contact is marked by channels which were cut into the Moenkopi formation prior to or during the deposition of the Shinarump sediments. These buried stream channels are, at the present time, the only major guide to uranium ore deposits in the Shinarump. All of the uranium deposits in the Shinarump of the Monument Valley area have been found in these buried channels, but not all channels contain mineralized zones.

These ancient buried channels in the Monument Valley area range in size from 10-20 feet wide and 5-10 feet deep to 200-2,000 feet wide and 70-200 feet deep.

FIELD METHODS

The Shinarump member of the Chinle formation in the areas included in this discussion ranges in thickness from a few feet to 200 feet. If the velocity contrast between the Moenkopi formation and Shinarump member is, on the average, 2 to 1, the total length of an individual spread should be about seven times the depth, so that the critical distance will be about one-half the total spread length or less. The most generally useful spread length is 550 feet, but spreads 1,100 feet long are used for the greater thicknesses of Shinarump; shorter spreads may be used where the Shinarump is very thin. In reconnaissance profiling, spreads are placed end to end; but, when channel areas are detailed, each succeeding spread overlaps the preceding one by 50 percent. Dynamite charges are fired at both ends of each spread. When drill holes are available, inhole velocity surveys, using detectors lowered into the drill-holes, are made to provide reliable vertical velocities.

Conventional 12-channel portable refraction seismic instruments, usually mounted in a light four-wheel drive vehicle, and conventional inline geophone spreads are used. Charges are fired both in the air and in shallow shot holes. The U. S. Geological Survey has used shovels and hand augers to dig shot holes, with dirt tamping; a jack-hammer was used by the Bureau of Reclamation. Although smaller charges can be used in shot holes, air shooting with single elevated charges has been used almost exclusively by the U. S. Geological Survey (with no loss in record quality) because of the saving in time and the elimination of much of the flying debris that accompanies refraction shooting in shallow holes. The area is thinly populated and air shooting brings few protests. Charges of from 2 1/2 to 10 pounds of 60 percent gelatin dynamite are fired from steel poles 3 to 6 feet high. Wooden 2 inch by 2 inch blocks are used to prevent damage to the shooting poles. The blocks contain drill holes which slide over the top of the steel pole and 1/2 inch sharpened wooden dowels on which the dynamite charges are placed. The charges are fired from a distance of about 200-300 feet after all metal bands have been removed from the dynamite. Small fragments of cap wire may be thrown for considerable distances and may cut cables placed too near a shot point. Safety precautions include use of safety hats for exposed field personnel, hanging the cap wire so that it will be blown away from the instrument truck, and placing the instrument truck between field personnel and the shot point.

Shot point and geophone locations and elevations must be determined by plane table or transit surveys.

A typical seismic refraction crew consists of party chief-interpreter, observer-shooter, surveyor, and three or four laborers.

INTERPRETATION

The classical methods of interpreting seismic refraction traveltime curves based on critical distance and intercept-time formulas, as outlined in the standard geophysical textbooks, yield misleading results in interpreting channel structures in Monument Valley. The erosional surface on the Moenkopi is not a plane surface; it is most irregular in the channel areas of greatest interest. The width of many (probably most) channels is less than a typical spread length, so the refracting interface must be considered as a curved surface. High-velocity mudstone lenses within the Shinarump in many places preclude accurate determination of the velocity in the Shinarump because the V_1 (Shinarump) portion of the traveltime curves will then represent, in whole or in part, the velocity in the mudstone and not the average velocity in the Shinarump; if thin lenses extend over entire spread lengths, use of the higher velocity in depth computations will yield erroneous depths. This is the familiar problem of velocity inversion. Lateral and vertical variations in the velocity in the Shinarump, caused by changes in the physical properties of the sandstone, also complicate the problem and require fairly close drill-hole control and velocity logging for complete interpretation. An increase in velocity is usually associated with thickening of the Shinarump.

Corrections

Routine weathering corrections should be made but this is seldom possible. The base of the weathered layer in Monument Valley is an indefinite boundary between the unweathered Shinarump at rather shallow depths and the overlying aerated Shinarump and residual or windblown soil. The water table is generally at very great depths, well below the Shinarump and Moenkopi contact. The weathered layer velocities are very low, in places 500 fps or less, so minor variations in the thickness of the weathered layer cause large arrival-time delays. It is seldom possible to make routine weathering corrections, however, because high-velocity mudstone lenses and other velocity variations in the Shinarump interrupt the continuity of the V_1 (Shinarump) segments of the traveltime curves. Thus, the recognition of variations in the thickness of the weathered layer, as opposed to variations in the depth to the Moenkopi, becomes a problem which is inseparable from the overall process of interpretation.

Arrival-time delays on the V_1 segment of a traveltime curve which are duplicated on the overlapping V_2 (Moenkopi) segment from the reversed shot can be identified as weathered-layer time delays. However, high-velocity mudstone traveltime segments at short distances from the shot point may make this distinction impossible. In such places, the arrival-time delays are revealed only on the V_2 segment, and they could be caused by either variations in the thickness of the weathered layer or the depth to the Moenkopi. Time variations caused by changes in the depth to the Moenkopi, however, will be displaced from the depth point away from the shot point on each of the reversed shots, and they will not coincide. Time variations caused by changes in the thickness of the weathered layer will coincide in horizontal position.

Elevation corrections are not made in the conventional manner for it is usually impossible to choose a flat datum that will be valid for any considerable distance. Computed depths are plotted on cross sections below the surface (or subweathering) elevations so that, in effect, elevation corrections are made graphically.

A typical manifestation of a thin mudstone lens within the Shinarump member is shown in figure 2. The difference between arrival time variations caused by variations in the thickness of the weathered layer and those caused by changes in the depth to the Moenkopi formation is illustrated by figure 3.

Delay time analysis

A modification of an interpretation procedure suggested by Barthelmes (Barthelmes, 1946; Dobrin, 1952, p. 237-240) is used in interpreting the curved refracting surfaces in channel areas. However, the classical refraction formulas can be used for preliminary analyses of refraction traveltime curves in Monument Valley. The procedure used involves calculating the "delay time" for each geophone and treating delay time variations as resulting from variations in the depth of the refractor. The delay time has been defined as the additional time required for a wave to travel any segment of a ray trajectory over the time that would be required for a wave to travel the horizontal component of that segment at the highest velocity reached by the trajectory (Nettleton, 1940, p. 250).

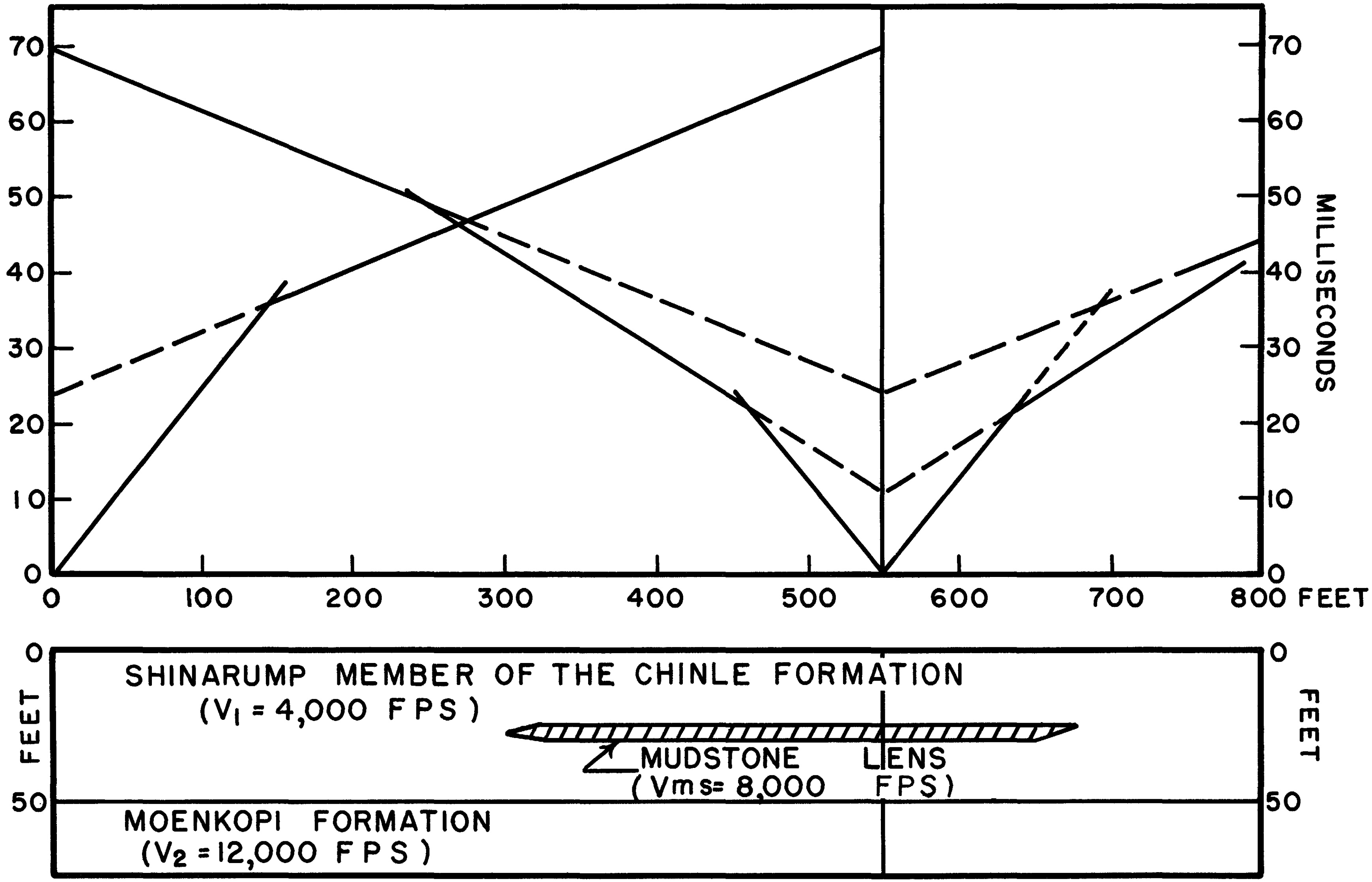

Figure 2. Effect of a mudstone lens on traveltime curves

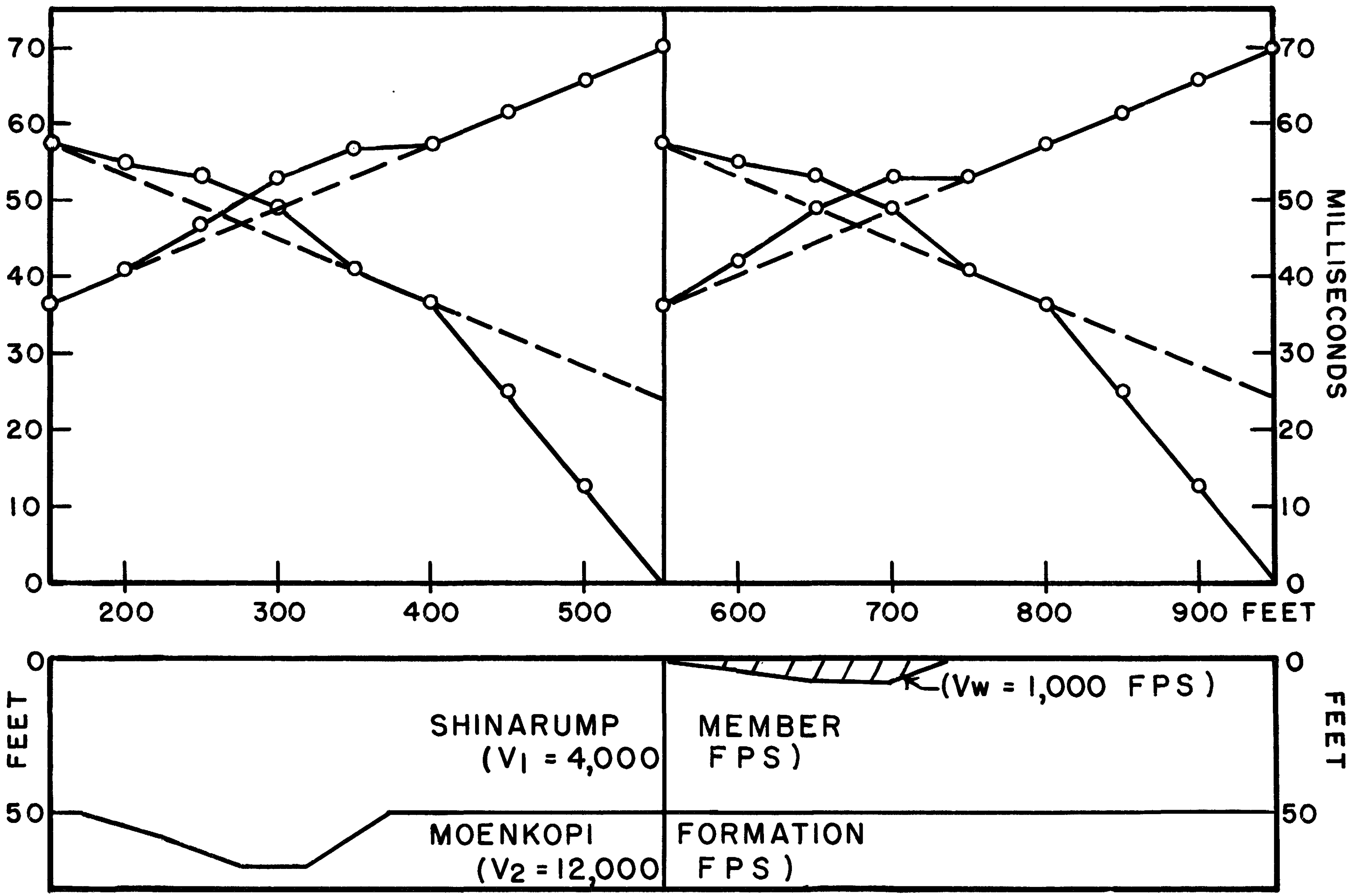

Figure 3. Effects of channel and change in weathered-layer thickness on traveltime curves

For a two-layer case without dip, the time taken by a wave to travel from the shot point to any detector beyond the critical distance is:

$t = x/V_2 + (2z \cos i)/V_1$, where

x is the horizontal distance from the shot point to the detector,

V_1 is the velocity of the overburden,

V_2 is the velocity of the deeper, high-velocity, layer,

z is the depth to the high-velocity layer, and

i is the critical angle of incidence ($\sin i = V_1/V_2$).

The sum of the delay time terminating at the shot point and any detector is $(2z \cos i)/V_1$. This is identical to the intercept time $(x = 0)$.

If the depths at the shot point and detector, either because of dip or surface elevation changes, are not equal, the traveltime from the shot point to any detector (see fig. 4) becomes:

$t = x/V_2 + (z_s \cos i)/V_1 + (z_d \cos i)/V_1$, where

z_s and z_d are the depths below the shot point and detector respectively, measured normally to the refracting interface.

The latter two terms of the equation are the delay times for the shot point and detector respectively. Therefore, the sum of the delay times for the shot point and any detector can be determined by subtracting x/V_2 from the detector arrival times. Because the delay time for the shot point remains constant for any spread, any variations in the delay time for detectors are proportional to variations in depths to the refractor beneath those detectors. The depth variation between

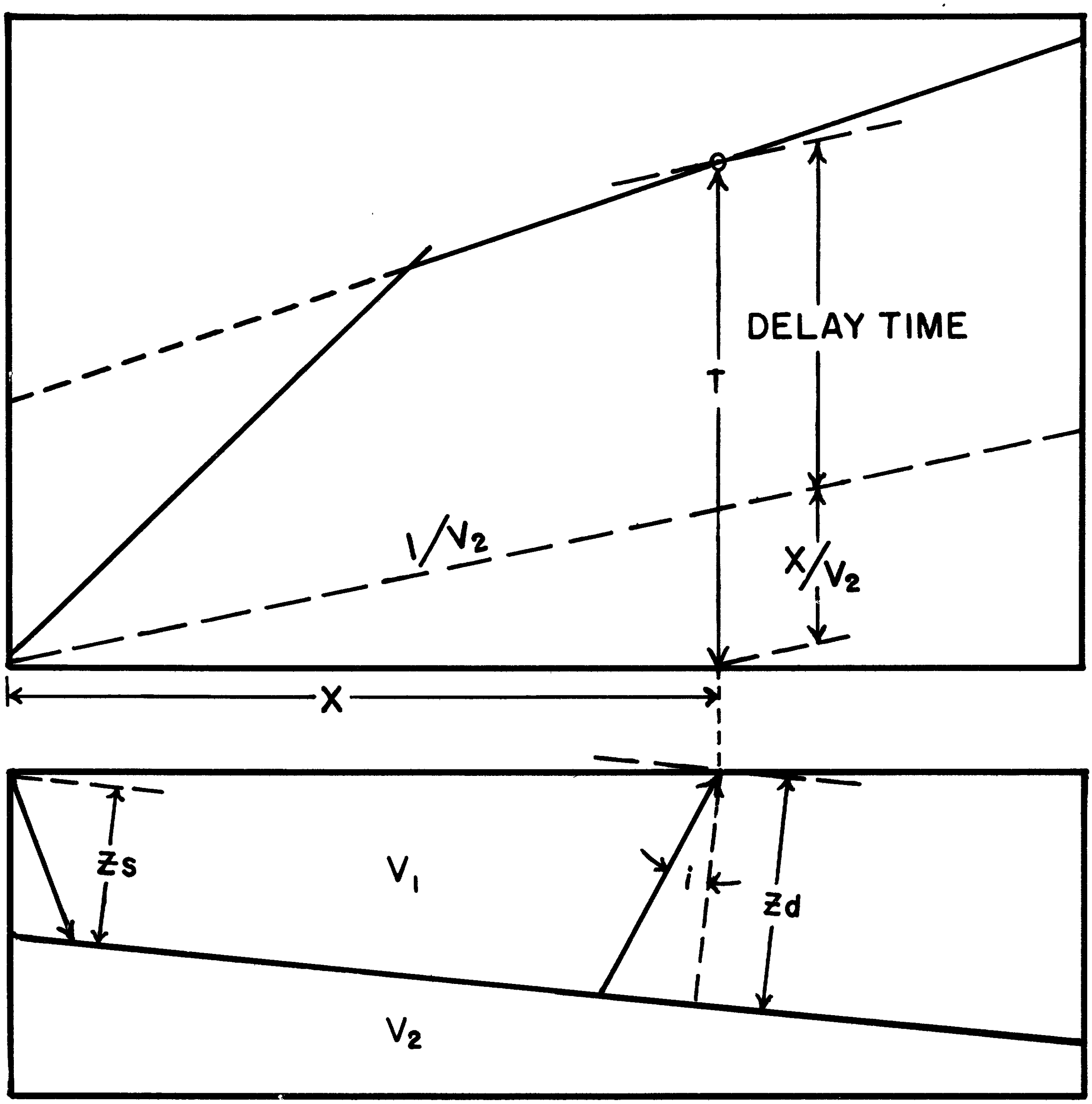

Figure 4. Graphical illustration of delay time

any two detectors is:

$\Delta z_d = (\Delta t_D V_1)/\cos i$, where

Δt_D is the difference in delay times between the two detectors. The depth point is not directly below the detector, however, but (ignoring dip) is displaced toward the shot point by:

$\Delta x = z_d \tan i$.

Thus it is possible to calculate the total delay time for the shot point and detector for each detector position and to calculate from those total delay times the depth variations. If the depth at any point is known (from a drill hole) or can be calculated at any shot point by the classical refraction formulas (that is, where the refractor is a plane surface), the depth at any other point can be determined by adding or subtracting the appropriate depth variation.

The following relationships also apply:

The delay times are equal for opposite ends of a reversed spread — that is, if the end detector is placed at the opposite shot point, $t - x/V_2$ will be identical for waves traveling from opposite ends of the spread because identical paths have been traveled.

The difference in delay times for waves arriving at any detector from two different shot points (usually, but not always, from opposite ends of a spread) is proportional to the difference in depth between the two shot points, or

$\Delta z_s = (\Delta t_D V_1)/\cos i$.

This is true because the delay times for the detector location are identical.

Procedure

The delay time method is used in practice in the manner described below (fig. 5).

1. Plot the traveltime curves for opposite ends of a reversed spread in the usual manner.

2. Through the origin, at each end of the spread, construct a line whose inverse slope is equal to the known velocity of the high velocity refractor. (This velocity may be determined from traveltime curves in an area where the surface of the refractor is a plane surface.)

3. Scale the time difference between each arrival time (beyond the critical distance) and the corresponding position on the sloping line constructed in Step 2, above. This is the total delay time and this step is equivalent to subtracting x/V_2 from the detector arrival times. The total delay time is equal to the sum of the delay times for the segments terminating at the shot point and detector.

4. Plot the total delay time so determined beneath each detector position. (Note that the time scale for delay times increases downward so that increases in depth are shown by downward deflections of the delay time curve.)

5. Migrate (the term "migrate" refers to the process of shifting a seismic depth point laterally from a position vertically below a shot point or detector to its true horizontal position (Hagedoorn 1954)) the position of the delay time for each detector position toward the shot point by:

$$\Delta x = z \tan i.$$

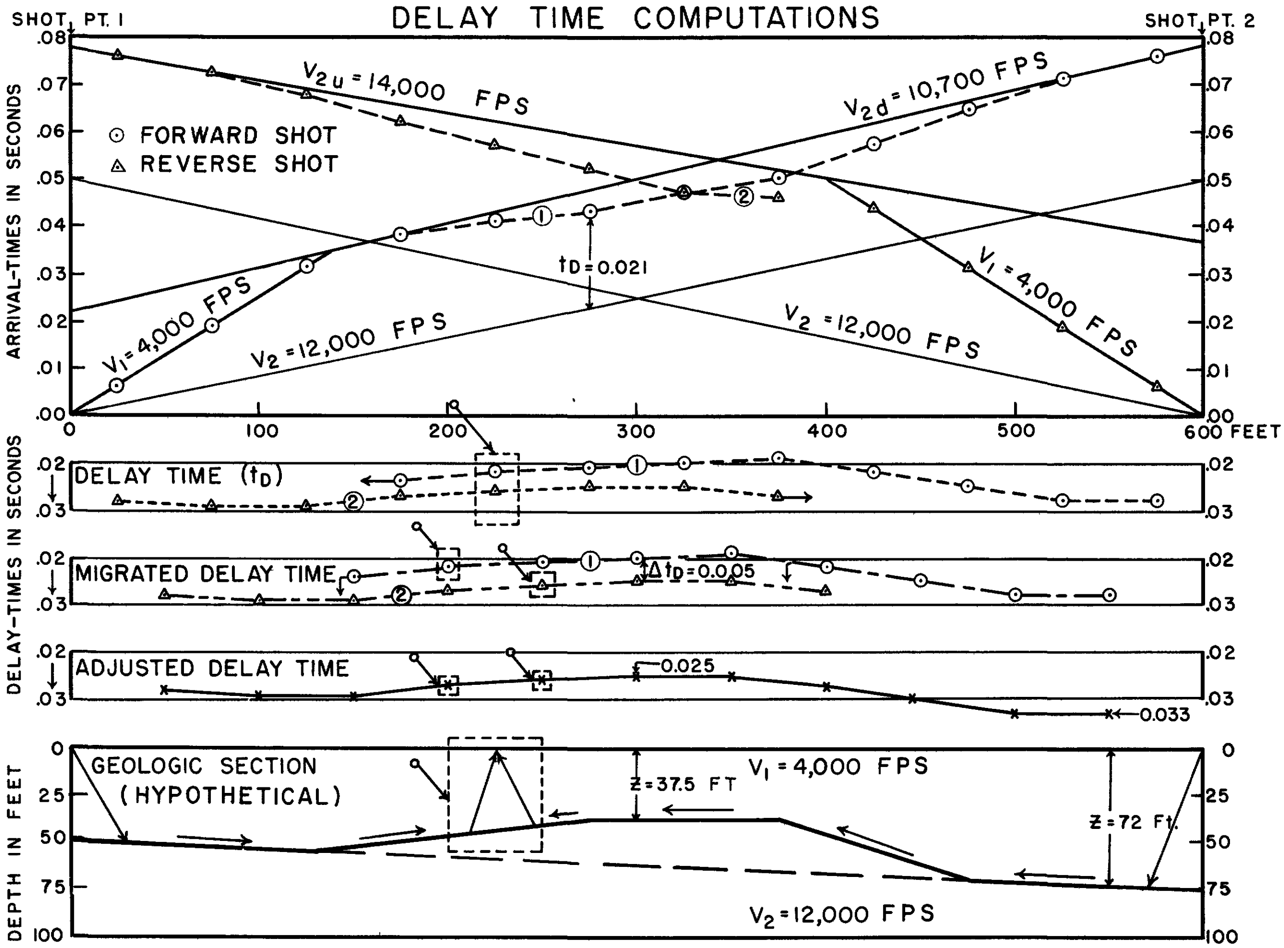

Figure 5. Graphical delay time analysis.

Actually, the amount of migration will change for each detector position if the depth changes. However, if the depth changes are not extreme no great error will be introduced if an average depth is assumed and all delay times are migrated the same distance on the same spread. The migrated delay times obtained from a shot point at one end of a spread will not be the same as those obtained from the shot point at the other end of the spread; they will differ by a constant amount that is proportional to the difference in depth of the refractor below the shot points. (See above.)

6. Scale and average the delay time differences for the forward and reverse shot for each detector position. Adjust the delay time curve by shifting one overlapping delay time curve upward or downward by this difference. The overlapping portion of the two delay time curves should now coincide if the proper velocity has been chosen. If it does not coincide, individual discrepancies should be averaged out; weathered-layer effects and delay time variations caused by local elevation irregularities should be removed. This process of shifting and averaging can be continued for any number of delay time curves overlapping each other. The delay time difference for waves traveling in the zone of overlap to a detector position from any two shot points, regardless of their directions or distances from the detector, will be proportional to the difference in depth between the two shot points.

7. Choose any point on the adjusted delay time curve as a datum (preferably a point at which the depth is known or can be easily determined). Determine the delay time difference of each detector position from this datum and calculate the corresponding depth difference

from:

$$\Delta z_d = \Delta t_D V_1 / \cos i.$$

The true depth for each detector position can then be determined by adding or subtracting this depth difference from the known depth. Even in the event that there is no known depth, or the traveltime curves are so irregular that a plane portion cannot be selected for a reliable computed depth, depth differences computed from the delay time differences will yield reliable relative depths.

8. Plot the depth or relative depth below the surface elevation at the appropriate detector position.

Figure 5 shows this process in its entirety. Note how the total delay time (t_D) of 0.021 seconds is determined by scaling the time difference between the arrival-time and the 12,000 fps line below. The delay times are shifted in the directions of the horizontal arrows to get the migrated delay time curves. One migrated delay time curve (marked 1) is shifted downward by 0.005 seconds to get the adjusted delay time curve, and it now coincides with the migrated delay time curve from the opposite shot point (marked 2).

The depth at the detector position nearest Shot Point 2 is calculated from:

$$z = t_D V_1 / 2 \cos i.$$

This point was selected because the delay time curve is flat here and the refractor must be nearly flat. The depth to the refractor can therefore be computed directly from the total delay time in a manner similar to the intercept time method.

The adjusted delay time for the detector nearest Shot Point 2 is 0.033 seconds. This is established as the datum. The delay time differences from 0.033 are determined and from them the depth differences are calculated.

When calculating the total depth the factor 2 is included in the denominator of the equation because delay times for both shot point and detector are included. When calculating depth deviations, it is omitted, for the delay time deviations relate only to the detectors.

It is seen that the errors involved in the assumption that all delay times may be migrated by the same amount are not great. The hypothetical geologic section from which the traveltime curves were derived and the adjusted delay time curve have the same appearance. The sharp changes in slope are smoothed out somewhat on the adjusted delay time curve.

Checking delay time curves

The graphical delay time interpretation method just described includes many approximations but it is possible to control the overall accuracy of the final delay time curve rather closely by the following checks:

1. The delay times for opposite ends of a reversed spread should be equal.

2. The difference in delay times for any detector for different shot points is proportional to the difference in depth of the high speed refractor between the two shot points.

3. If overlapping delay time curves are not parallel, the assumed high velocity is in error and it can be corrected. Variations in the velocity of the high velocity layer (Moenkopi) can be detected by this means.

4. The difference in time on the adjusted delay time curve between any two shot points must be equal to the difference in delay times of the overlapping migrated delay time curves for those two shot points. This is the amount one curve must be shifted to obtain coincidence.

These relationships can be used to "tie" the adjusted delay time curve between shot points, or to "bridge" gaps in zones where overlap of the migrated delay time curves is inadequate or absent.

EXAMPLES

Where mudstone lenses are present in the Shinarump the traveltime curves may appear to be standard three-layer plots. A typical series of traveltime curves and two possible interpretations of the data are shown in figure 6. The first interpretation assumes spreads 1 and 3 to be two-layer plots and spread 2 to be a three-layer plot. Standard two- and three-layer computations were made using the critical distance method. The second interpretation assumes that the intermediate velocity of spread 2 is caused by refraction from a thin mudstone lens within the Shinarump. The depth computations were made by extending the V_1 portion of spread 2 to intersect the V_3 portion of the traveltime curves and treating the problem as a two-layer case, ignoring the V_2 portion altogether. The second interpretation fits the local geologic conditions much better than does the first interpretation.

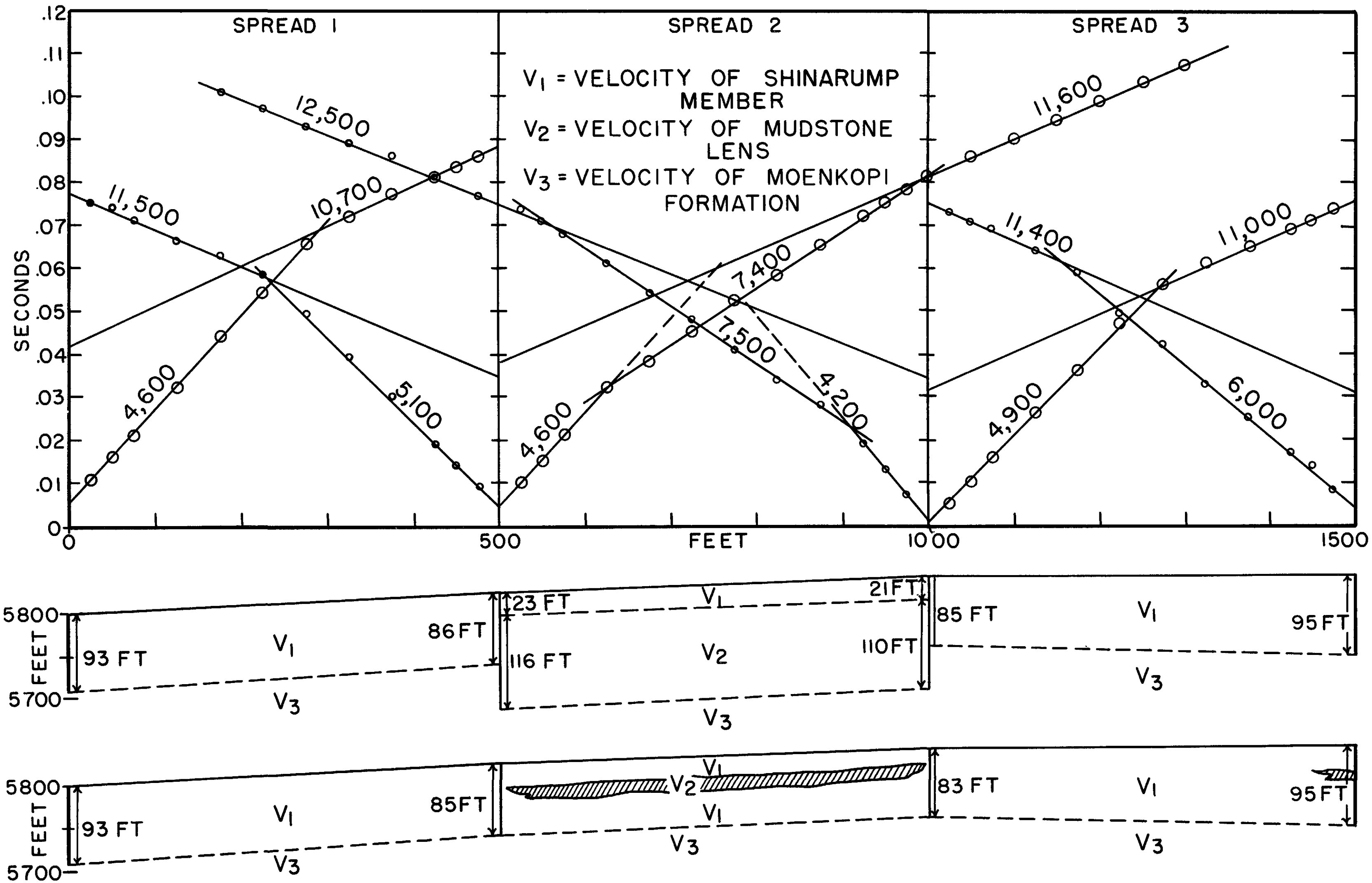

Figure 6. Graphical illustration of possible misinterpretation caused by mudstone lens

Some error is involved in ignoring mudstone lenses. However, if we assume that the velocities of the Shinarump, mudstone lenses, and Moenkopi are 4,000, 7,000, and 12,000 fps respectively, and that ignored mudstone lenses account for 25 percent of the Shinarump thickness, the error in the computed depth to the Moenkopi will be less than 10 percent, and relative depths will be accurate.

Actual inhole velocity measurements made in drill holes in the Shinarump of Monument Valley are shown in figure 7.

The delay time method of analysis offers a means of extracting the most information from the seismic data. In many places, where a seismic spread spans a channel width, the delay time method of analysis will show the presence of a channel that would remain undetected by standard computation methods. Figure 8 illustrates this situation. Here the traveltime curves appear to indicate that the Shinarump and Moenkopi contact is relatively flat. In reality this spread crosses a channel, although not in a direction normal to the channel axis. The velocities of 15,500 fps as shown on the traveltime curves are apparent velocities indicating upslope travel along the refractor immediately below the V_2 segment for each shot point. This slope reversal reveals the presence of the channel and it is readily detected by the delay time analysis using a Moenkopi velocity of 13,000 fps.

In some places the presence of a buried channel is indicated on the traveltime curves, even without the use of delay times. In figure 9 the traveltime curves for the center spread show definite evidence of channeling which is borne out by the delay time analysis. The assumed Moenkopi velocity of 12,000 fps is apparently in error for the spread to the left. Depths computed at each shot point by the

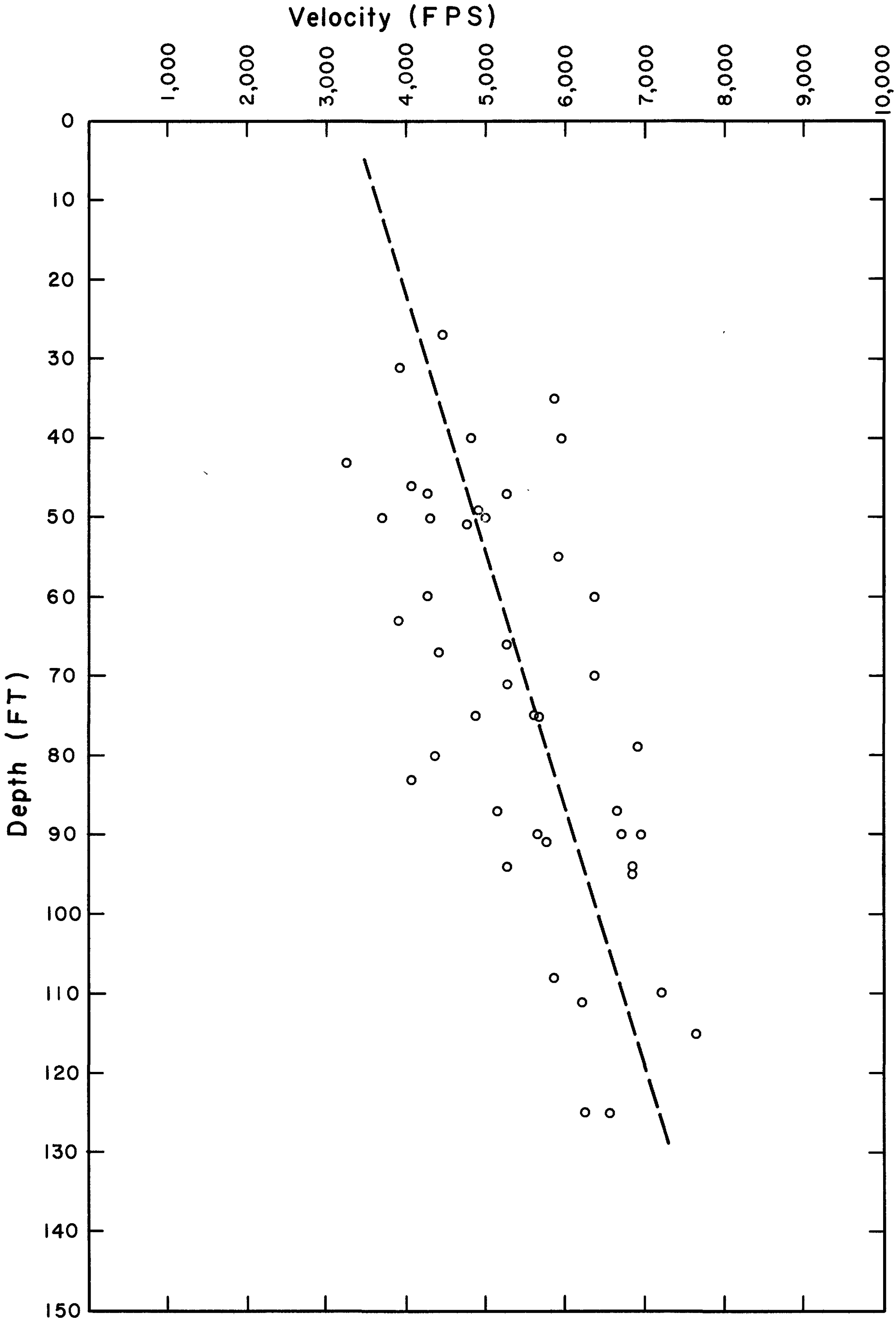

Figure 7. Inhole velocity measurements in the Shinarump from selected drill holes in a typical Monument Valley area

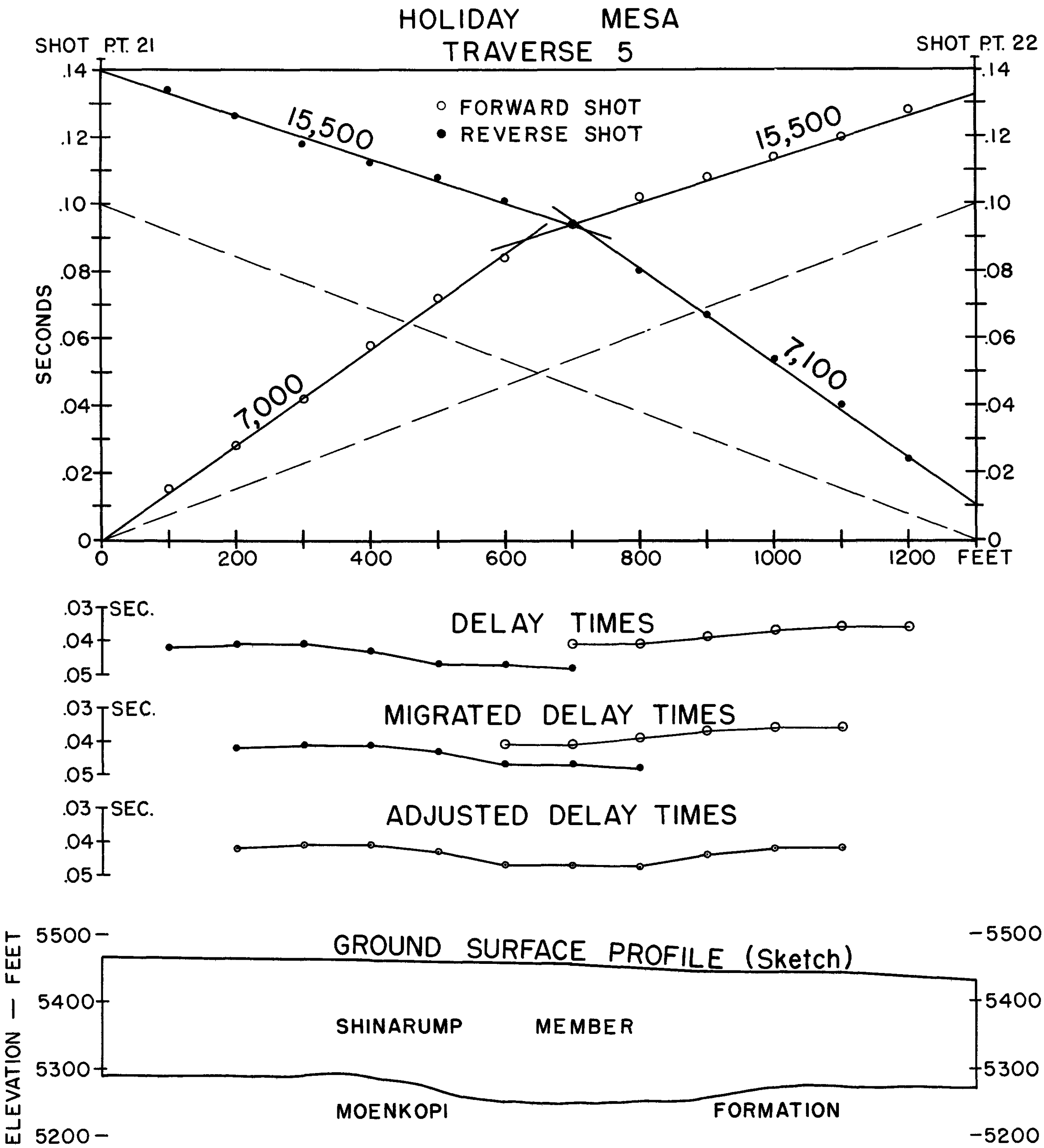

Figure 8. Channel revealed by delay time analysis

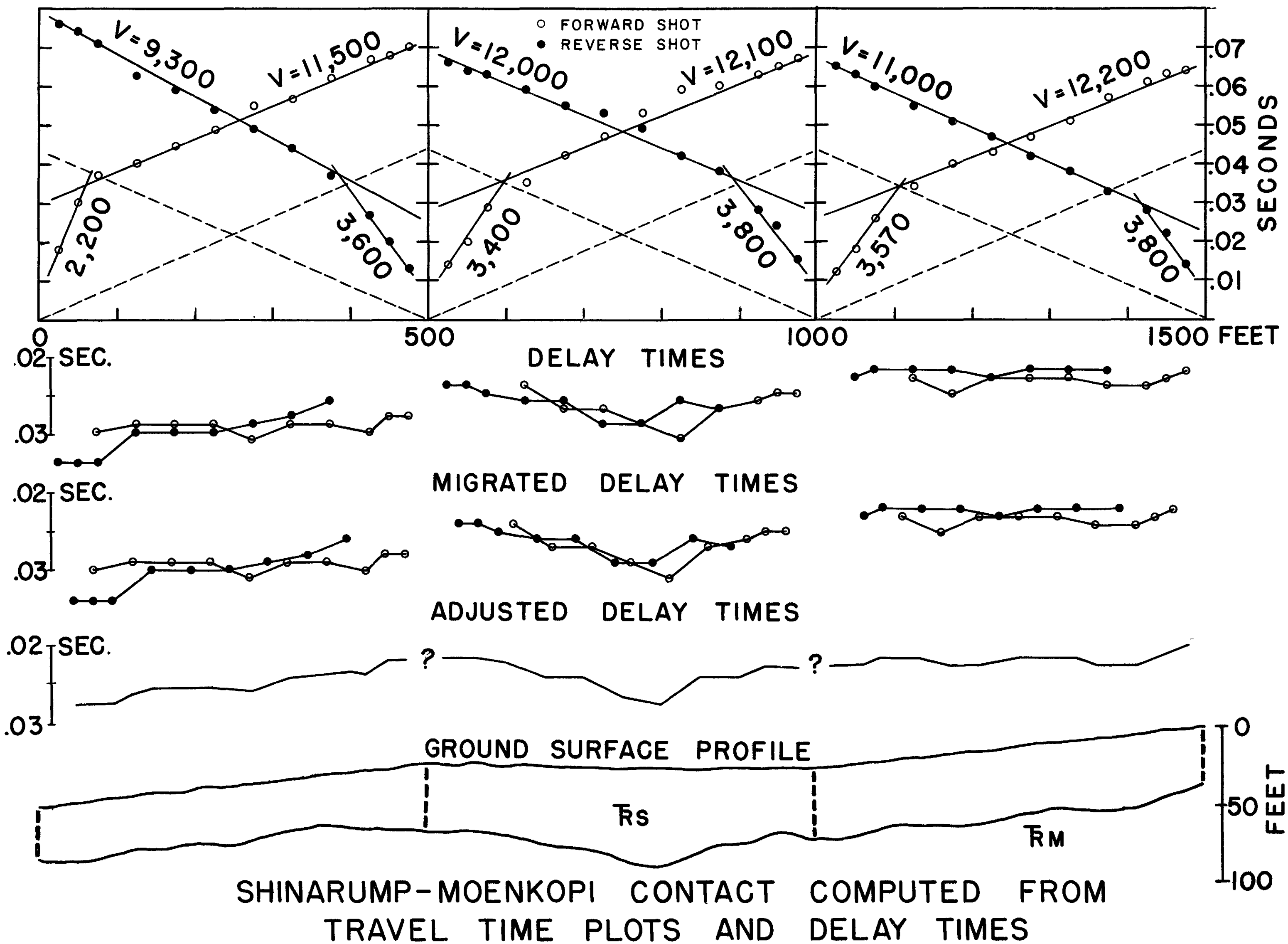

Figure 9. Typical delay time interpretation.

classical formulas were used here for control.

Where complete overlap is obtained, it may be possible to tolerate fairly large errors in the assumed V_2 by averaging the delay time curves from opposite directions, just as it is permissible to average apparent updip and downdip velocities for a dipping bed where the dip is not too great. This procedure can lead to serious discrepancies, however, where the assumed velocity is greatly in error, or if the process is extended too far from one pair of overlapping delay time curves to the next, and it is not recommended. In figure 10a the assumed Moenkopi velocity was in error and the migrated delay time curves were not parallel (solid lines). When the velocity was corrected the migrated delay time curves became parallel (dashed lines). There is virtually no difference in the adjusted delay time curves, however. But in figure 10b the adjusted delay time curves for the assumed and corrected velocities differ markedly. The correct adjusted delay time curve (dashed line) indicates the presence of a small channel that might otherwise be overlooked.

The seismic refraction method will not reveal the presence of all buried channels. In some places mudstone will nearly fill the channel scour and, as shown in figure 11, the top of the mudstone will be mapped instead of the bottom of the channel scour. Parallel profiles where mudstone is missing will reveal the channel.

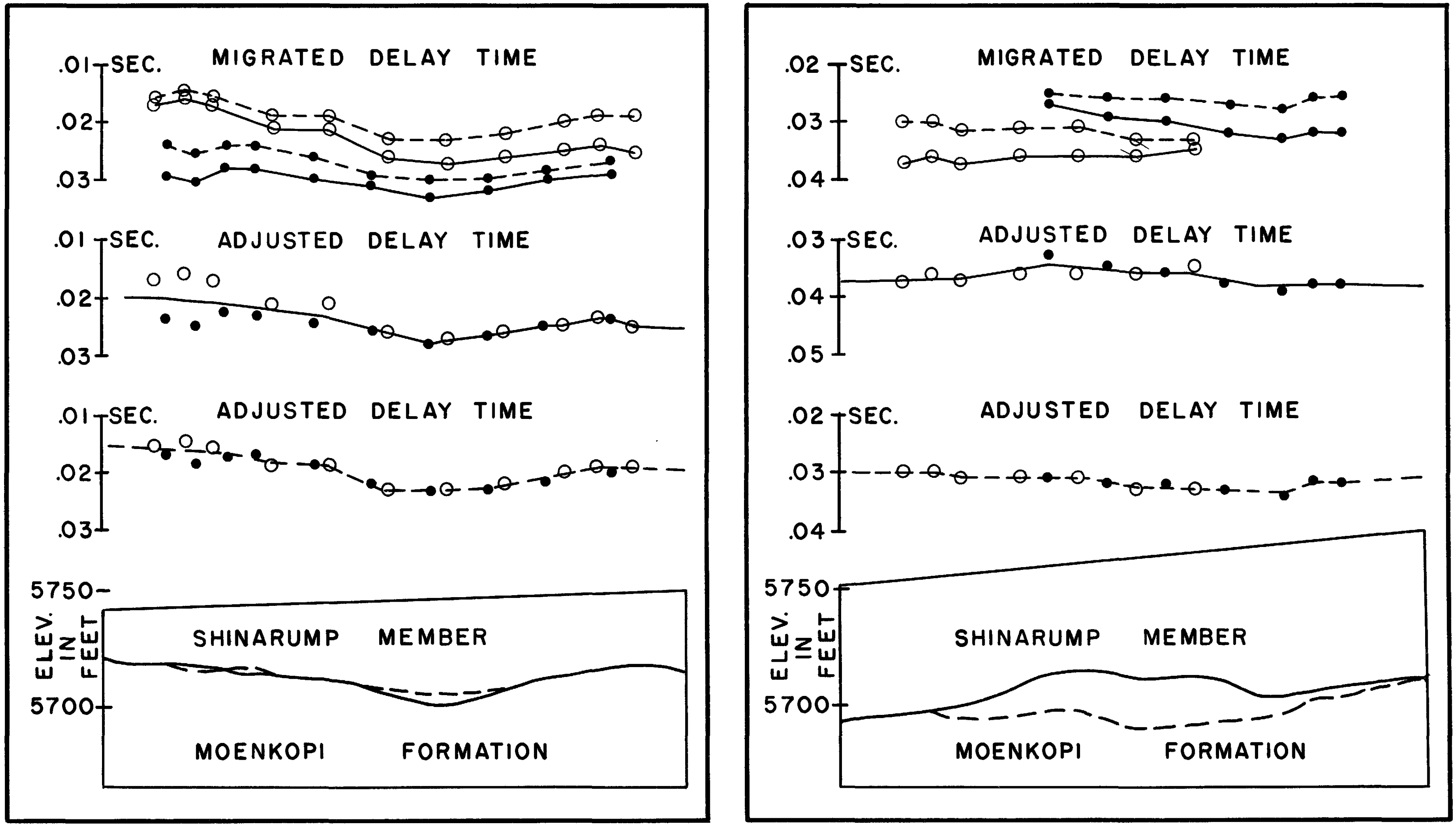

Figures 10a and 10b. Effects of erroneous velocities in the Moenkopi. (Solid lines show delay times obtained from erroneous velocities in the Moenkopi; dashed lines delay times for corrected velocities. Conventions for forward and reverse shots same as fig. 8)

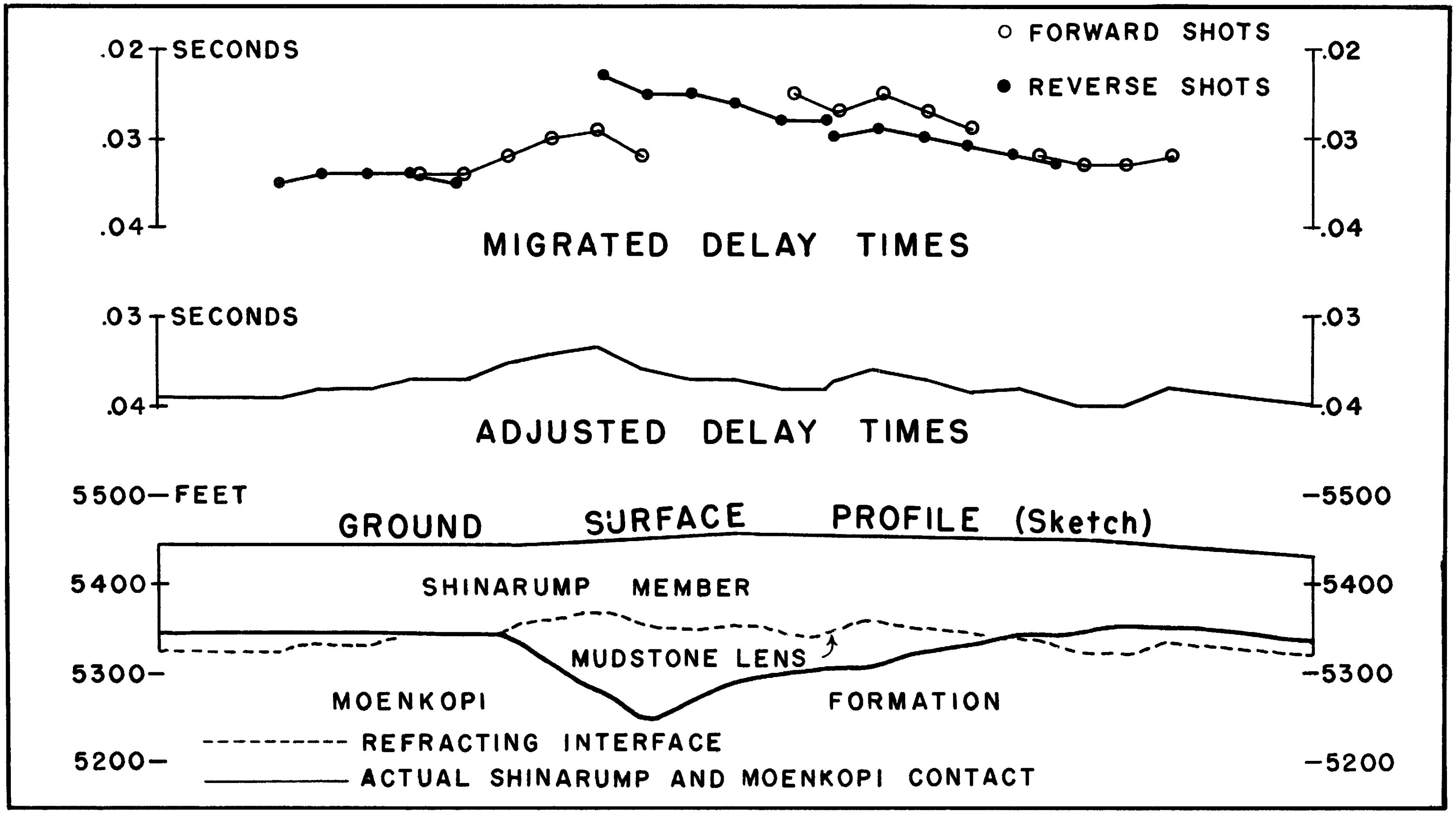

Figure 11. Effect of mudstone lens in channel on delay time interpretation

CONCLUSIONS

The refraction seismograph is a useful tool in the discovery of ancient channels in the Monument Valley area of Arizona and Utah. These channels, cut into the Moenkopi formation by stream action and filled with the basal sediments of the Shinarump, may localize important accumulations of uranium ore in the Shinarump. Exploratory drilling in channels discovered with the refraction seismograph must be relied upon, of course, actually to find uranium ore. The seismic refraction method, using portable jeep-mounted instruments (which can be readily removed for operations in inaccessible areas), is cheap and reliable. It is at present the most successful geophysical method of locating channels used by the U. S. Geological Survey.

Many difficulties in interpretation not anticipated in routine seismic refraction operations are found in exploring for ancient channels, but these difficulties can be overcome by imaginative use of the methods outlined in this paper.

LITERATURE CITED

Baker, A. A., 1936, Geology of the Monument Valley-Navajo Mountain region; San Juan County, Utah: U. S. Geol. Survey Bull. 865, 106 p.

Barthelmes, A. J., 1946, Application of continuous profiling to refraction shooting: Geophysics, v. 11, no. 1, p. 24-42.

Dobrin, Milton B., 1952, Introduction to geophysical prospecting: 435 p. New York, McGraw-Hill Book Co.

Hagedoorn, J. G., 1954, A process of seismic reflection interpretation: Geophys. Prosp., v. 2, no. 2, p. 7-127.

Nettleton, L. L., 1940, Geophysical prospecting for oil: 444 p. New York, McGraw-Hill Book Co.

Wantland, Dart, 1954, Examples of geophysical exploration for uranium: Mines Mag., v. 44, no. 9, p. 26-33.

Wantland, Dart, and Casey, R. D., 1952, Field tests for the United States Atomic Energy Commission on the use of the seismic geophysical method for tracing "buried channels" in the Monument Valley area, Arizona: U. S. Bur. Reclamation Geology Rept. G-123, 68 p., issued by U. S. Atomic Energy Comm. Tech. Inf. Service, Oak Ridge, Tenn.